Human Molecular Genetics, 2013, Vol. 22, No. 7 **1432–1442**
doi:10.1093/hmg/dds560
Advance Access published on January 9, 2013

Contribution of growth differentiation factor 6-dependent cell survival to early-onset retinal dystrophies

Mika Asai-Coakwell[1], Lindsey March[2], Xiao Hua Dai[1], Michele DuVal[2], Irma Lopez[6], Curtis R. French[1], Jakub Famulski[2], Elfride De Baere[7], Peter J. Francis[8], Periasamy Sundaresan[9], Yves Sauvé[1,3], Robert K. Koenekoop[6], Fred B. Berry[4,5], W. Ted Allison[2,4], Andrew J. Waskiewicz[2,*] and Ordan J. Lehmann[1,4,*]

[1]Department of Ophthalmology, [2]Department of Biological Sciences, [3]Department of Physiology, [4]Department of Medical Genetics, and [5]Department of Surgery, University of Alberta, Edmonton, Canada T6G 2H7, [6]McGill Ocular Genetics Laboratory and Pediatric Ophthalmology, McGill University Health Centre, Montreal, QC, Canada H3A 1A1, [7]Center for Medical Genetics, Ghent University Hospital, Ghent, Belgium, [8]Casey Eye Institute-OHSU, Portland, OR 97239, USA and [9]Aravind Eye Hospital, Madurai 625 020, India

Received December 5, 2012; Revised December 5, 2012; Accepted December 27, 2012

Retinal dystrophies are predominantly caused by mutations affecting the visual phototransduction system and cilia, with few genes identified that function to maintain photoreceptor survival. We reasoned that growth factors involved with early embryonic retinal development would represent excellent candidates for such diseases. Here we show that mutations in the transforming growth factor-β (TGF-β) ligand *Growth Differentiation Factor 6*, which specifies the dorso-ventral retinal axis, contribute to Leber congenital amaurosis. Furthermore, deficiency of *gdf6* results in photoreceptor degeneration, so demonstrating a connection between Gdf6 signaling and photoreceptor survival. In addition, in both murine and zebrafish mutant models, we observe retinal apoptosis, a characteristic feature of human retinal dystrophies. Treatment of *gdf6*-deficient zebrafish embryos with a novel aminopropyl carbazole, P7C3, rescued the retinal apoptosis without evidence of toxicity. These findings implicate for the first time perturbed TGF-β signaling in the genesis of retinal dystrophies, support the study of related morphogenetic genes for comparable roles in retinal disease and may offer additional therapeutic opportunities for genetically heterogeneous disorders presently only treatable with gene therapy.

INTRODUCTION

Evolutionarily conserved signaling pathways [transforming growth factor-β (TGF-β), Wnt and Hedgehog] pattern the embryo (reviewed in 1); however, our understanding of their contribution to human disease remains incomplete (2,3). One challenge is that early embryonic developmental phenotypes occlude analysis of later gene functions, even though signaling pathway cassettes are utilized repeatedly during development, and mutations cause both early- and late-onset disease. The 20 bone morphogenetic proteins (BMPs) and growth differentiation factors (GDFs) that comprise one TGF-β ligand subfamily (4) perform core roles in axis formation, cell fate determination and patterning (5–7). As either homo- or hetero-dimeric ligands (8–10) BMP/GDFs activate SMAD phosphorylation (reviewed in 11), as well as multiple non-canonical pathways [mitogen-activated protein kinase, Rho-like GTPase and phosphatidylinositol-3-kinase/AKT (12)]. Although initially identified through an ability to induce bone and cartilage formation (13) targeted BMP inactivation revealed far wider developmental roles (14), with those in visual development closely paralleling embryonic patterning (15). In ocular morphogenesis, BMP/

*To whom correspondence should be addressed. Tel: +1 7804924403 (A.W.), +1 7804928550 (O.L.); Fax: +1 7804929234 (A.W.), +1 7804926934 (O.L.); Email: aw@ualberta.ca (A.W.), olehmann@ualberta.ca (O.L.)

GDFs specify dorsal fate (16) by activating dorsal targets *Tbx5*, *Aldh1a2* and *Efnb2*, whilst simultaneously repressing ventrality genes, *Vax2* and *Ephb2* (17,18). Opposing the effects of BMPs, Sonic hedgehog specifies ventral identity (19). In the last few years, GDFs have been shown to sub-serve comparable functions, with Gdf6 positioned at the top of the known hierarchy of retinal genes specifying the dorso-ventral retinal axis (20–22). In zebrafish (20) and *Xenopus* (8), Gdf6 initiates dorsal retinal identity, is expressed prior to Bmp4 and lies genetically upstream of dorsal retinal patterning genes [*bmp4*, *bmp2b* and *tbx5* (21,22)].

On the basis of its role patterning the vertical axis of the developing retina, we hypothesized that *GDF6* mutation would underlie a spectrum of retinal disease. We uncovered evidence that zebrafish Gdf6 plays a role in later eye development, notably that *gdf6* mRNA is expressed in the proliferative ciliary marginal zone with apoptotic cell death observed in mutants. Guided by these new data demonstrating a connection between Gdf6 function and retinal cell proliferation/survival, we selected Leber congenital amaurosis (LCA) [OMIM: 204000], the most severe inherited retinal dystrophy for analysis. LCA is a clinically and genetically heterogeneous group of disorders, characterized by profound congenital visual loss, nystagmus and absent full-field electroretinogram (ERG) responses. Representing a common cause of congenital blindness (prevalence, 1 in 30 000–50 000), it is typically autosomal recessively inherited (review in 23). To date, mutation of 20 genes account for ~65% of LCA [including: phototransduction (*GUCY2D*); retinoid cycle (*LRAT*, *RPE65*, *RDH12*); cell maintenance (*AIPL1*, *TULP1*, *RD3*); ciliary function (*CEP290*, *IQCB1*, *LCA5*, *RPGRIP1*); retinal development (*CRB1*, *OTX2*, *CRX*) and NAD biosynthesis (*NMNAT1*)]. A subset (*RPE65*, *SPATA7*, *RPGRIP1*, *CRB1*, *CEP290*, *LRAT*, *CRX*, *RDH12*) also contribute to more common and later-onset retinal dystrophies—retinitis pigmentosa [RP (MIM 180100)] or cone-rod dystrophy [CRD (MIM 180020)] (24–28).

Human, murine and zebrafish analyses were employed to demonstrate involvement of one *GDF* ligand in early-onset retinal dystrophies. As the first TGF-β signaling pathway member associated with retinal dystrophies, this defines an entirely new mechanism for onset of such disorders. It also implicates other paralogs as leber congenital amaurosis or retinitis pigmentosa (LCA or RP) candidates, and the data presented illustrate that mutation of a second *GDF* ligand induces comparable phenotypes. Retinal apoptosis was evident in two animal models, and observation of its inhibition with a novel chemical compound may provide additional opportunities for clinical translation (29,30).

RESULTS

To examine the role of *GDF6* in severe retinal dystrophies, DNA samples from 279 LCA and juvenile retinitis pigmentosa (JRP) patients were screened for mutations affecting the two exons of *GDF6*. This revealed in one proband, a compound heterozygous mutation, c.169G>C and c.746A>C, resulting in amino acid changes p.57D>H and p.249A>E (31), respectively (Fig. 1A). The proband, whose vision is limited to detection of hand motions, exhibited the extinguished ERG typical of the LCA phenotype (Fig. 1B). This individual does not have other ocular or systemic phenotypes, but has not undergone the radiological imaging necessary to detect milder *GDF6*-induced skeletal disease. The proband's parents each carried a single *GDF6* variant and exhibited specific ERG abnormalities [reduced b-wave amplitude (paternal) and delayed rod b-wave implicit time (maternal) (Fig. 1B)], comparable with those observed in carriers of LCA mutations (32). Three additional heterozygous GDF6 amino acid alterations were identified in the LCA/JRP cohort: p.E292D (c.876G>A—pedigree II), p.A199T (pedigree III) and again p.A249E (pedigree IV) (Fig. 1C); variants that were either absent from control chromosomes (D57H and E292D: 0 of 1500, A199T: 0 of 650) or present at a low prevalence (A249E: 4 of 1500). Two of these are known mutations that induce either ocular (A249E: microphthalmia, coloboma; A199T: severe colobomatous microphthalmia with foveal hypoplasia) (31,33) or skeletal disease (A249E: postaxial polydactyly, Klippel-Feil) (34,35); however, such phenotypes were not observed in the LCA/JRP patients.

To assess the effects of GDF6 variants on function, we analyzed protein levels and secretion in transfected COS7 cells. These revealed that, compared with wild-type protein levels, the amounts of GDF6-A249E pre-pro-protein and mature ligand were reduced in the media (36 and 53%, respectively). A marked reduction in the levels of GDF6-D57H pre-pro-protein and mature ligand were observed in both cytosolic (80 and 97%) and media (97 and 99%) fractions, with co-transfection of both GDF6-A249E and -D57H showing reduced mature ligand in the media (27% decrease), but not cell lysate (Supplementary Material, Fig. S1). To assess growth factor activity, we utilized reporter constructs containing two BMP response elements (BREs) from the *1d1* promoter fused to a luciferase reporter (36). Quadruplicate assays, performed on three separate occasions, demonstrated that GDF6-A249E and GDF6-D57H activated the reporter at 50 and 24% of the GDF6-WT activity [$P < 0.001$, Student's *t*-test (Fig. 1D)]. These data support a model whereby compound heterozygosity for A249E and D57H significantly compromises GDF6 activity.

Next we assessed *in vitro* the functional effect of amino acid alterations discovered in LCA patients with one wild-type and one putatively defective *GDF6* allele. These heterozygous GDF6 variants revealed increased levels relative to wild-type protein in the whole-cell lysate [full length: GDF6-E292D, 37% increase; GDF6-A199T, 47%] and media fractions [mature ligand: GDF6-E292D, 56%; GDF6-A199T, 4%] (Fig. 2A). In contrast to our expression data, reporter assays demonstrated significantly reduced activation of BRE-luciferase by these variants compared with GDF6-WT (E292D 69% decrease, A199T 56%, $P < 0.005$, Student's *t*-test) (Fig. 2B). These functional assays support the heterozygous E292D and A199T alterations also contributing to LCA.

To evaluate the effect of mutations in a murine model, $Gdf6^{tm1Lex}$ mice (MGI ID: 3604391) with targeted deletion of *Gdf6* exon 2, hereafter referred to as $Gdf6^{+/-}$, were crossed to yield homozygous progeny. Since none was generated from 15 litters [$Gdf6^{+/+}$ $n = 39$, $Gdf6^{+/-}$ $n = 64$], analysis was undertaken at E18 revealing genotypes more reflective of Mendelian ratios [$Gdf6^{+/+}$ $n = 4$, $Gdf6^{+/-}$ $n = 6$, $Gdf6^{-/-}$ $n = 5$; from three pregnancies]. Accordingly,

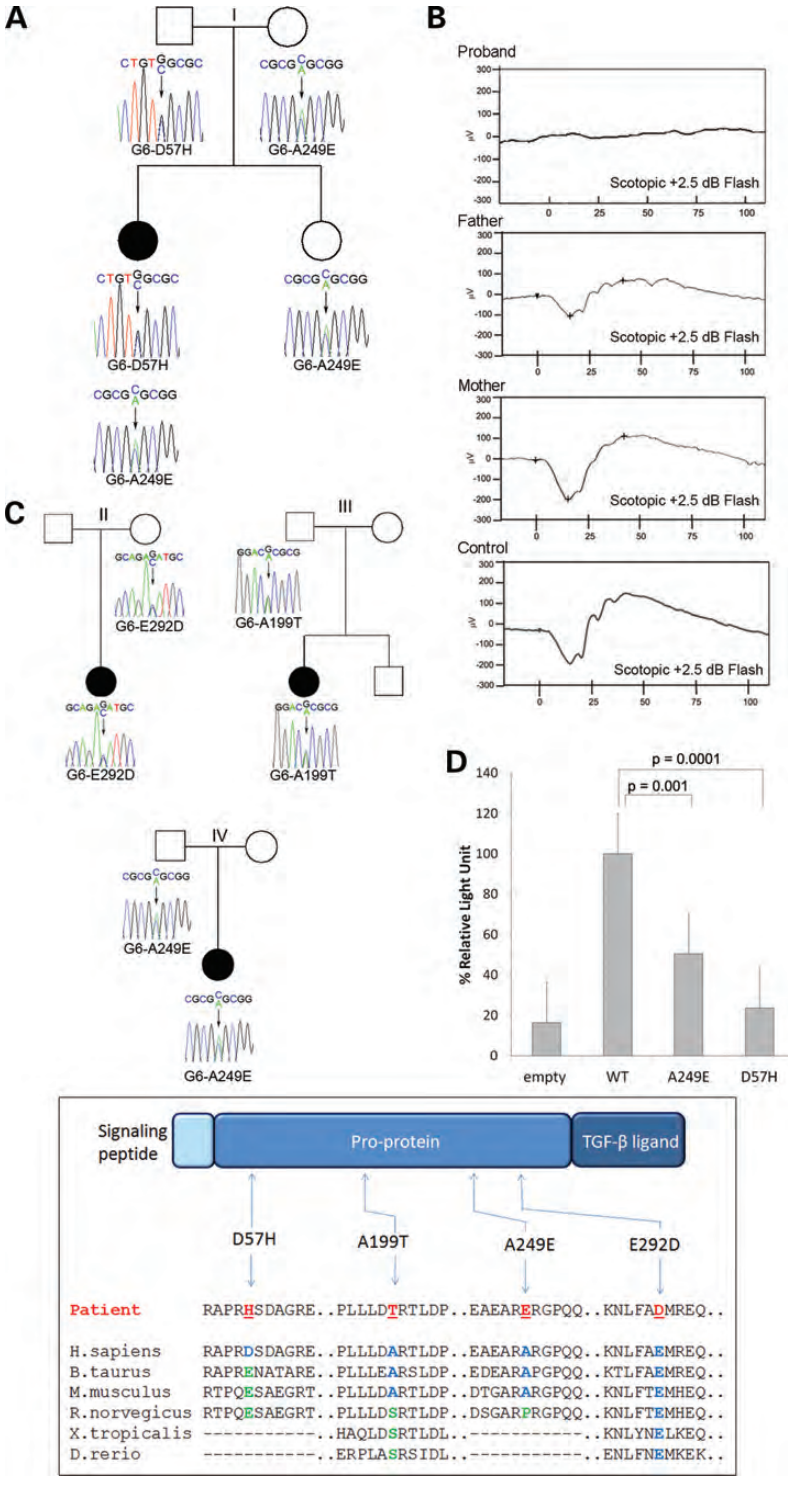

Figure 1. *GDF6* mutations identified in LCA and JRP pedigrees are associated with phenotypic and functional consequences. (**A**) In contrast to the proband with two GDF6 mutations (D57H and A249E), the unaffected parents and sibling carry single variants. (**B**) Scotopic ERG recordings from the same pedigree demonstrate the proband's extinguished ERG and subtle parental ERGs anomalies [paternal: reduced b-wave amplitude; maternal: delayed rod b-wave implicit time; control (below)]. (**C**) Three additional heterozygous *GDF6* mutations, E292D (II), A199T (III) and A249E (IV) detected in LCA/JRP pedigrees. (**D**) BRE luciferase reporter analysis demonstrates significantly decreased transactivation by transfected variants (GDF6-A249E or GDF6-D57H) when compared with GDF6-WT [data represent the mean of 12 replicates (error bars, SD, $P \leq 0.001$, *t*-test)]. Inset below, GDF6 protein domain structure with amino acid alignment of missense mutations in LCA and JRP patients (ClustalW).

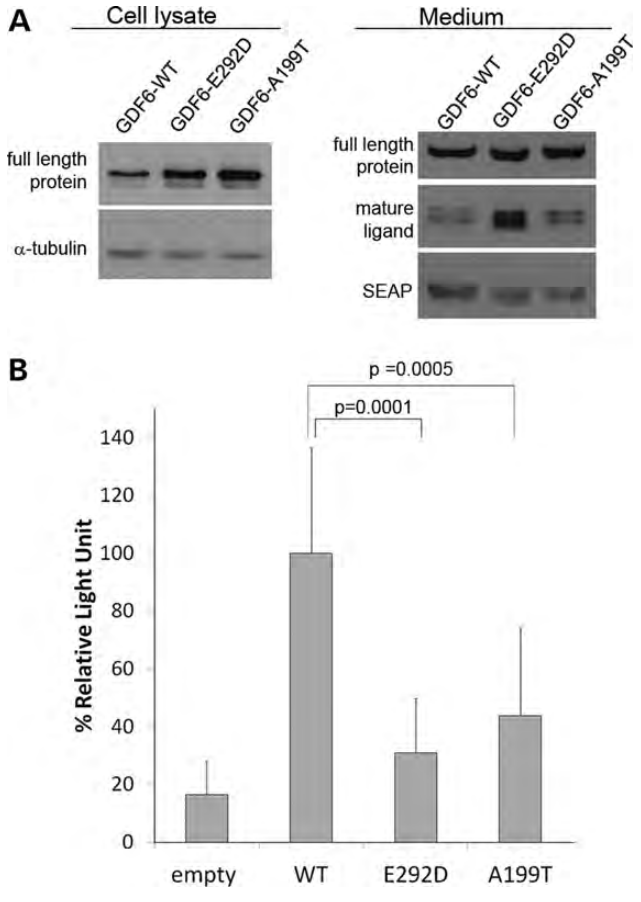

Figure 2. Evidence of altered biochemical function for heterozygous GDF6 variants. (**A**) Western blot analysis demonstrated increased levels of E292D and A199T mature ligand compared with wild-type in the cell media. (**B**) Luciferase reporter analysis revealed decreased activation of the 2xBRE reporter for both variants compared with wild-type (error bars, SD; $P \leq 0.0005$, *t*-test). Alpha tubulin and secreted alkaline phosphatase (SEAP) represent controls for cytosolic and secreted proteins, respectively.

ERGs were recorded in adult heterozygous mutants ($Gdf6^{+/-}$) and wild-type ($Gdf6^{+/+}$) littermates ($n = 12$). A subset of $Gdf6^{+/-}$ mice (five of nine) exhibited abnormal ERGs with up to 66% decreases in the bipolar cell driven b-wave [pure cone (saturated photopic) and mixed rod-cone (saturated scotopic) (Supplementary Material, Fig. S2)] and 54% decreases in the photoreceptor mediated a-wave amplitudes. The more pronounced reductions of the b-wave than a-wave amplitudes accord with preferential inner retina changes observed in heterozygous patients [parents of LCA probands (Fig. 1B) and others, described below] (32). Reduced photopic flicker fusion (3–27%), another indicator of inner retinal dysfunction, was also observed in the same five $Gdf6^{+/-}$ mice. Such findings are compatible with a role for Gdf6 in murine and human retinal function.

In view of the biochemical evidence that human GDF6 variants were functionally significant (Figs 1 and 2, Supplementary Material, Fig. S1), and the typically autosomal-recessive nature of LCA and JRP, using exomic next-generation sequencing, we tested the hypothesis that a second TGF-β variant was present in probands with a single *GDF6* mutation. However, due to extreme GC-content, exome sequencing yielded incomplete coverage across the open-reading frames of BMP ligands (data not shown), preventing identification of the known heterozygous mutations and precluding testing of our hypothesis. In parallel, to determine whether mutation of other TGF-β members alters retinal function consistent with a contribution to retinal dystrophies, we examined a pedigree with a well-characterized mutation (GDF3-R266C) in a paralog with significant roles in retinal development. Notably, *GDF3* mutation results in near identical ocular and skeletal phenotypes to *GDF6* (31,34). The hypomorph studied increases the number of highly conserved cysteine residues in the mature ligand (Supplementary Material, Fig. S3A), and compared with wild-type *GDF3* reduces luciferase activation by ∼50% (34). Each GDF3-R266C heterozygous carrier exhibited abnormal ERGs with decreased scotopic b-wave amplitudes, and variable phenotypic severity that is characteristic of human BMP-induced ocular and skeletal phenotypes (29,37,38). Notably, one individual had nearly extinguished scotopic and photopic waveforms with amplitudes <10% of normal (Supplementary Material, Fig. S3B) findings consistent with other members of the TGF-β superfamily contributing to retinal dystrophy phenotypes.

Collectively, the above data demonstrate an increased prevalence of GDF6 variants in LCA/JRP cases with a disease role supported by the appreciably altered biochemical function, and the ERG anomalies observed with heterozygous mutation of a close paralog. Intrigued by these observations, we sought to analyze the consequence of long-term loss of Gdf6 function on retinal and photoreceptor structure. We turned to zebrafish, given the ease with which we could study homozygous mutants and the availability of a strain containing a p.S55X stop codon mutation ($gdf6a^{s327/s327}$, hereafter called $gdf6a^{-/-}$) (21). Viable homozygous mutants were generated by twice outcrossing to strain AB, with genotypes confirmed by sequencing (Fig. 3A). Examination of adult $gdf6a^{-/-}$ mutants revealed microphthalmia, with eyes obscured by overgrown skin (Fig. 3A) and dissection revealing misshapen irides (Fig. 3B). Histological analysis of $gdf6a^{-/-}$ mutants at 2 weeks of age demonstrated profound alterations to the morphology of individual photoreceptor subtypes [Red/green cones (Fig. 3C and D) and UV cones (data not shown)]. Studies at later timepoints revealed loss of normal retinal lamination, as evident from actin and nuclear stains (Fig. 3E and F), together with appreciable disorganization of Müller glia cells, as assessed by glial fibrillary acidic protein (GFAP) immunohistochemistry (Fig. 3E–H). The increased GFAP abundance in $gdf6a^{-/-}$ adult eyes (Fig. 3F) is consistent with the gliosis common to neurodegenerative diseases and animal models thereof (39). Finally, in $gdf6a^{-/-}$ adults, cone photoreceptors were consistently dysmorphic and reduced in abundance (Fig. 3I–L).

Since photoreceptor death is a key feature of retinal dystrophies, the level of apoptosis was determined during mouse and zebrafish embryogenesis. At E18, a stage at which the murine retina is divisible into neuroblastic and ganglion cell layers, TUNEL-positive cells were observed in both (Fig. 4A–F) with increased levels of apoptotic signal observed in $Gdf6^{-/-}$ and $Gdf6^{+/-}$ mice compared with wild-type [mean TUNEL-positive cells/section: $Gdf6^{-/-}$ 30.4; $Gdf6^{+/-}$ 12.9; $Gdf6^{+/+}$ 8.3; $P = 0.016$ and $P < 0.0001$, Student's *t*-test

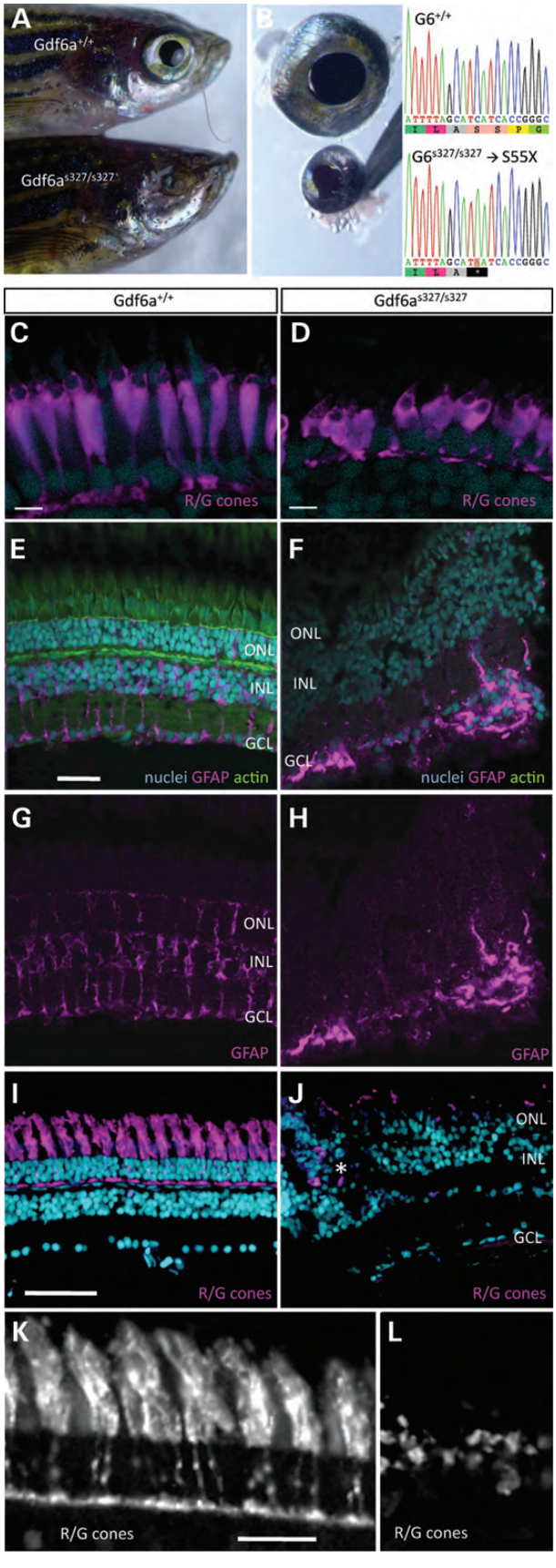

(Fig. 4G)]. Substantially increased apoptosis was observed in the retinas of mutant fish compared with wild-type at 28 hpf [mean α-active caspase-3 signals/eye: *gdf6*$^{-/-}$ 76.4, WT 3.34 ($P < 0.0001$, ANOVA)] (Fig. 4H and K). Comparable findings were observed using acridine orange to observe apoptotic cells (40). Intrigued by observing increased embryonic retinal apoptosis in murine and zebrafish models of an LCA associated gene, we next evaluated in *gdf6*$^{-/-}$ mutants, whether this effect could be ameliorated with a novel anti-apoptotic compound, P7C3. This aminopropyl carbazole is reported to be pro-neurogenic, protecting newborn hippocampal neurons from apoptosis (41). P7C3 treatment of *gdf6*$^{-/-}$ embryos resulted in significantly reduced levels of retinal apoptosis at 28 hpf [70 and 79% reductions at 0.01 and 0.1 μM doses, respectively, $P < 0.0001$, ANOVA (Fig. 4I–M)]. Notably, this effect, evident in replicate experiments, was more pronounced at higher P7C3 concentrations (Fig. 4N). In light of P7C3′′s inhibition of *gdf6*$^{-/-}$ retinal apoptosis, we next assessed whether there was evidence of functional rescue, utilizing two distinct assays. The first [visually mediated background adaptation (VBA) (42)] is a neuroendocrine response in which the detection of ambient light by retinal ganglion cells results in melanosome contraction (43). Mutants exhibited increased pigmentation on a light background that was unchanged with dimethyl sulfoxide (DMSO), but it partially recovered with P7C3 treatment [*gdf6a*$^{-/-}$: DMSO 1 of 22 contracted melanophores; P7C3 11 of 22; *gdf6a*$^{+/+}$ 25 of 25 (Fig. 5)]. The second assay [optomotor response (OMR)] records the distance travelled in the direction of motion of a perceived stimulus. This motion evoked assay requires substantially higher levels of retinal sensitivity and is dependent on both visual (photoreceptor and retinal interneuron) and musculo-skeletal function. In contrast to the VBA result, OMR analysis did not reveal any improvement in response by *gdf6a*$^{-/-}$ mutants with P7C3 treatment (Supplementary Material, Fig. S4).

DISCUSSION

Perturbed TGF-β signaling in retinal dystrophies

We report that mutations in *GDF6* are associated with early-onset retinal dystrophies and present comparable findings from both zebrafish and murine *Gdf6* mutants. By demonstrating involvement in neuronal survival, these data extend

Figure 3. Adult homozygous gdf6a mutant zebrafish exhibit retinal degeneration. (**A**–**B**) Adult gdf6a$^{-/-}$ zebrafish have small eyes and dysmorphic pupils compared with wild-type [genotypes confirmed by sequencing (right)]. Immunohistochemistry at 2 weeks of age demonstrates that compared with wild-type, Red/Green cone photoreceptor morphology is profoundly altered with significant shortening of the cone inner segment (**C**, **D**). In adult fish, there is an inflammatory response in the form of abundant GFAP immunoreactivity, and lack of retinal polarization consistent with neurodegeneration in adult gdf6a$^{-/-}$ zebrafish (**F**, **H**) compared with wild-type (**E**, **G**). Both rod and cone photoreceptors are dysmorphic and decreased in adult gdf6a$^{-/-}$ zebrafish (**J**, **L**) compared with wild-type (**I**, **K**). [ONL/INL, outer/inner nuclear layer; GCL, ganglion cell layer; GFAP, GFAP; R/G, red/green cones (scale bars 5 μm)].

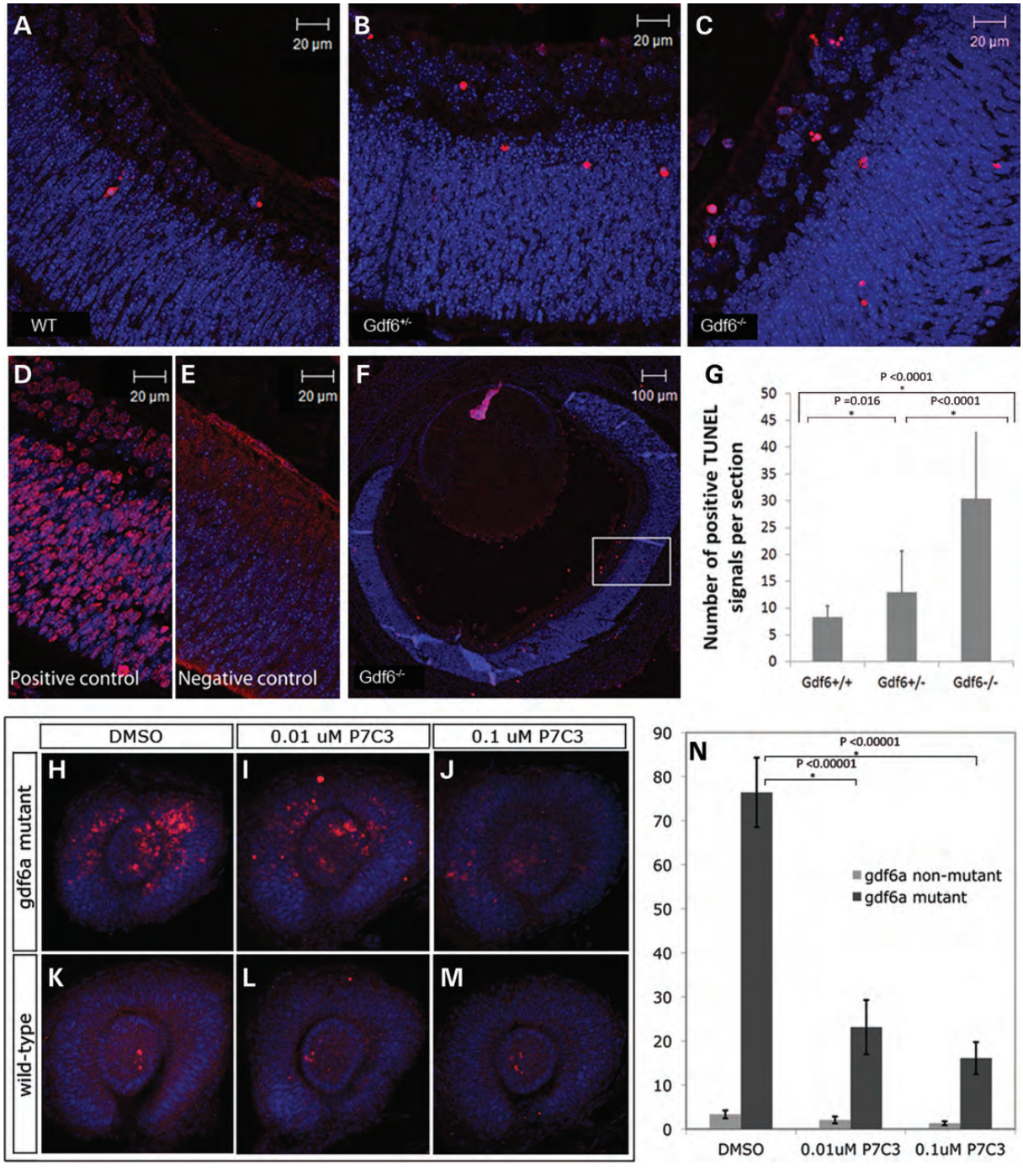

Figure 4. Gdf6 murine and zebrafish mutants demonstrate retinal apoptosis. (**A**–**F**) Montage of wild-type, Gdf6$^{+/-}$ and Gdf6$^{-/-}$ retinal sections illustrating the level of TUNEL-positive (red) signals in the neuroblastic layer (NBL) and ganglion cell layer (GCL) of E18 murine embryos [Hoechst (blue) co-staining]. In contrast to the low level of apoptosis in wild-type retina (**A**), higher levels are evident in heterozygous (**B**) and homozygous (**C**) mutant embryos [positive (**D**) and negative (**E**) controls]. (**F**) Low-magnification of entire Gdf6$^{-/-}$ retinal cross section to show localization of TUNEL-positive cells [boxed area shown at higher magnification in C]. (**G**) The progressive, and statistically significant, increase in the total number of TUNEL-positive signals with increasing Gdf6 null allele dosage is depicted graphically ($P < 0.05$, *t*-test). (**H**–**M**) Immunofluorescence with α-active caspase-3 antibody (red) and Hoechst (blue) in 28 hpf embryos. *gdf6a* mutant retinas display increased apoptosis (**H**) when compared with non-mutant siblings (**K**). Treatment with P7C3 reduces the amount of apoptosis in gdf6a mutant retinas (I and J) when compared with similarly treated non-mutant siblings (**L** and **M**). (**N**) Quantification of the number of anti-active caspase-3-positive cells in the retina showed non-mutant siblings treated with dimethyl sulfoxide (DMSO), 0.01 μM P7C3 and 0.1 μM P7C3 displayed a mean of 3.34 ($n = 44$), 2.07 ($n = 58$) and 1.32 ($n = 112$) apoptosing cells. *gdf6a* mutants treated as above displayed a mean of 76.41 ($n = 34$), 23.13 ($n = 16$) and 16.09 ($n = 33$) apoptosing cells, respectively. Error bars, SE; $^{*}P < 0.00001$ (ANOVA). All embryos included in statistics were genotyped via sequencing as being *gdf6a* mutants or wild-type siblings.

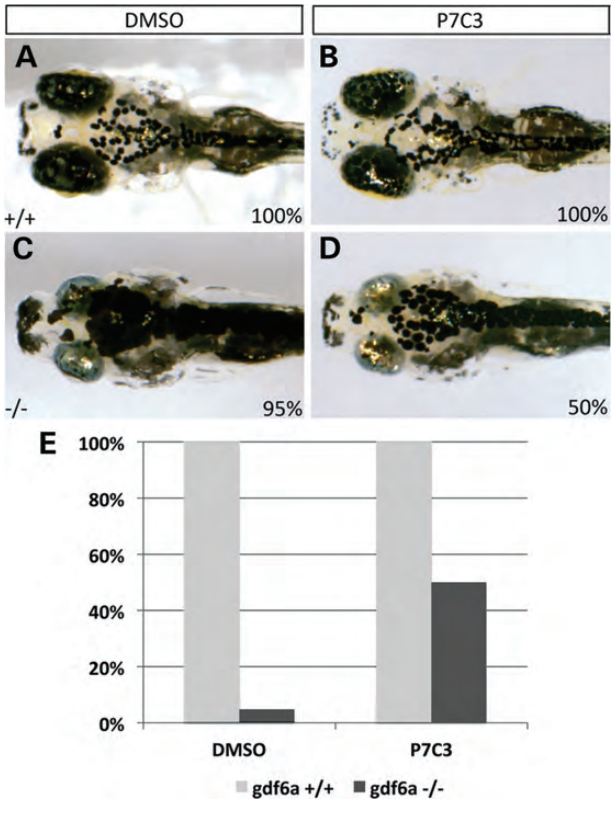

Figure 5. P7C3 treatment recovers visual background adaptation (VBA) activity in *gdf6a* mutant embryos. (**A**–**D**) Dorsal images of gdf6a mutant (−/−) and non-mutant siblings (+/+) treated with a control dose of DMSO (**A**, **C**) or 0.01 μM P7C3 (**B**, **D**). Larvae are 7 dpf in all panels. The contribution of the presented phenotype in each panel is indicated. DMSO- and P7C3-treated $gdf6a^{+/+}$ larvae have normal melanophore contraction (A, 100%, $n = 25$, *B*, 100%, $n = 24$) while DMSO-treated $gdf6a^{-/-}$ larvae have unresponsive VBA and widely distributed melanophores (*C*, 95%, $n = 21$). Treatment of $gdf6a^{-/-}$ larvae with P7C3 partially recovers VBA and melanophores appear partially contracted (D, 50%, $n = 22$). (**E**) Graph of the proportion of embryos that present fully or partially responsive VBA under the indicated conditions.

understanding of Gdf6 function from early retinal specification, involving for the first time TGF-β superfamily members in retinal dystrophies. Implication of *GDF6*, and through characteristic ERG anomalies, a second TGF-β member (Supplementary Material, Fig. S3), will catalyze evaluation of this gene family in molecularly unexplained LCA/JRP, particularly for variants in those paralogs with major retinal developmental functions. Since these phenotypes accord closely with Gdf6's specification of the dorso-ventral retinal axis, evaluating retinal morphogenetic genes for comparable disease contributions is merited, especially those specifying naso-temporal retinal identity [FGFs 3, 8, 18 and 19 (37,44,45)].

Despite the numerically small proportion of cases, GDF6's evolutionarily conserved role provides insight at several levels. The first relates to variants with significantly reduced biochemical function, where phenotypic effects are only detected in a proportion of heterozygotes on targeted testing (ERGs). This illustrates the eye's value as a genetic disease model, with electrophysiological testing revealing clinically silent retinal phenotypes, and causative alleles contributing to the singleton LCA cases that have proved recalcitrant to genetic elucidation (Fig. 1). Observation that 50% decreases in GDF6 signaling are tolerated while either compound heterozygous human (A249E and D57H), or homozygous murine or zebrafish null alleles induce severe phenotypes indicate that a threshold level of BMP signaling exists below which phenotypes manifest in all three species. This is supported by the progressively higher levels of retinal apoptosis with increasing null *Gdf6* allele dosage (Fig. 4G). The therapeutic corollary of observing disease phenotypes at high but not low mutational loads is that therapy only has to increase BMP signaling above this threshold (and not to 100%) to be effective.

The second feature concerns the elevated level of heterozygous functional *GDF6* variants in LCA/JRP cases (Figs 1 and 2). These are individually insufficient to induce LCA/JRP since the heterozygous parents are overtly unaffected, as are heterozygous murine and zebrafish mutants. However, their increased prevalence, the heterodimerization (46) and retinal developmental functions of other BMP/GDFs (34,38,47–49) plus the ERG anomalies of *GDF3* heterozygotes, all support the presence of additional disease-causing variants. Notably, the phenotypes caused by *Gdf3* and *Gdf6* mutation are very similar, with each inducing delayed choroidal fissure closure or coloboma, retinal developmental anomalies and axial skeletal patterning defects in patients and or model organisms (22,31,34,47,50,51). The presented data demonstrate that mutation of other BMP/GDFs induces retinal dysfunction, including extinguished ERGs that phenocopy the effect of *GDF6* mutation (Supplementary Material, Fig. S3), and will facilitate determining whether multi-allelic inheritance of BMP/GDF variants results in sporadic early-onset retinal dystrophies. An intriguing finding in this study was pleiotropy, with mutations (A249E) that cause postaxial polydactyly, Klippel-Feil or microphthalmia/anophthalmia/coloboma (MAC), only associated with LCA/JRP. This is explicable by buffering of disease phenotypes by the numerous ligands and BMP pathway members, leading to context-specific epistasis (52). Coupled with stochastic events, and recently identified compensatory autocrine and/or paracrine processes (53), such mechanisms likely account for the paradoxical ocular phenotypes.

Inhibition of Gdf6-induced apoptosis

TGF-β ligands are multifunctional cytokines that provide positional information to cells and control numerous aspects of their development. The profoundly altered cone morphology induced by *gdf6* mutation (Fig. 3), accords with this role and the patient LCA/JRP phenotype. In addition, these ligands have important pro- and anti-apoptotic functions (54–61), with the consistent, pan-retinally increased apoptosis of murine and zebrafish homozygous mutants revealing a fundamental and evolutionarily conserved requirement for Gdf6 in maintaining retinal cellular populations. This finding accords with the progressive apoptotic photoreceptor loss and increasing visual impairment characteristic of retinal dystrophies (62), and is evident in species with different proportions of cone photoreceptors (murine 3%, zebrafish 30%). Subsequent efforts concentrated on evaluating whether this neuronal loss was tractable to treatment (41). To date, the applicability of

anti-apoptotic agents has frequently been restricted by their broad mechanisms of action, which include inhibition of fundamental physiological processes. The significantly reduced activated caspase-3 signaling in P7C3 treated *gdf6*$^{-/-}$ mutants provides immunohistochemical evidence of rescue for a zebrafish LCA model. The paradoxical visual function results are derived from mechanistically distinct assays with log unit differences in sensitivity and involvement of different retinal cell types. Coupled with the known lenticular and skeletal phenotypes of *gdf6*$^{-/-}$ mutants (22,31), such factors may affect OMR but leave VBA unchanged, potentially explaining the differences between the datasets. In this context, P7C3's inhibition of neuronal apoptosis without deleterious effects in different tissues of evolutionary disparate species [murine CNS (41) and zebrafish retina], merits further investigation, especially as an effective anti-apoptotic agent (63) may synergize with other therapeutic approaches for enhancing neuronal survival (29,30,64).

Clinical and developmental implications

Of the key conclusions that can be drawn from GDF6's contribution to early-onset retinal dystrophies, the first relates to an invariant feature of BMP signaling from Drosophila to humans—exquisitely precise spatial and temporal regulation at multiple levels [including heterodimerization with other BMPs, antagonists and agonists, receptor and co-receptor expression, and Smad phosphorylation (65–69)]. Reinforcement of one ligand's signaling by another is a common paradigm, as exemplified by Gdf6a's induction of *bmp2b* and *bmp7a* transcription (70) leading to enriched BMP mRNA levels in specific regions of the developing embryo. Accordingly, it is improbable that involvement of TGF-β members in retinal dystrophies is confined to *GDF6*, as our *GDF3* data demonstrate. A second conclusion relates to the human ocular phenotypes induced by BMP mutation that have to date been restricted to alterations in ocular size (microphthalmia or anophthalmia) and tissue morphogenesis (coloboma) (31,33,34,50,71–73). This study significantly extends these roles, suggests that the MAC spectrum overlaps with retinal dystrophies and provides a simple means of testing this through ERG recordings of microphthalmia patients. In parallel, it implies a more complex interplay than hitherto appreciated between retinal and globe development, with broader implications for common disorders of ocular size (myopia and hyperopia). A third feature relates to this study's implication of a growth factor in LCA, which contrasts with the photoreceptor-specific nature of most LCA/JRP-causing genes. Finally, one consequence of seemingly disparate clinical disorders being caused by alterations to the same developmental pathway is that therapeutic approaches may benefit a range of disorders. In this context, the finding that BMP-induced apoptosis can be inhibited with P7C3 may lead to new approaches for treating disorders that still destine the vast majority of patients to visual impairment or blindness.

MATERIALS AND METHODS

Patient analysis

Two hundred and seventy-nine DNA samples from LCA or JRP patients, previously screened for mutations in the known causative genes, were polymerase chain reaction (PCR) amplified for *GDF6* and the products sequenced on an ABI Prism 3100 capillary sequencer (Applied Biosystems) (as previously described) (31). Chromatograms were analyzed using Sequencher (vs 4.5, GeneCodes) with amino acid sequence alignments performed using ClustalW (http://www.genome.jp/tools/clustalw/). The prevalence of mutations in western Canadian population control samples was determined by restriction enzyme analysis [*BsrBI* (A249E), *HaeII* (D57H), *HgaI* (A199T), *NlaIII* (E292D) (New England Biolabs)] ($n =$ 462 DNA samples) and direct sequencing of both exons ($n =$ 288 samples). Collection and analysis of DNA samples was approved by the University of Alberta Hospital Health Research Ethics Board, with informed consent provided by all participants.

Western blot and luciferase assays

Wild-type *GDF6* transcript was generated by PCR of genomic DNA, cloned into pCR4-TOPO (Invitrogen, ON, Canada) and mutations introduced by site-directed mutagenesis. Subcloning into pcDNA3.2/V5-DEST (Invitrogen) or CS2^{+} was undertaken for western blot and luciferase analyses, respectively (31). Western blots were performed on lysates collected 48 h after transiently transfecting wild-type GDF6 or the individual variants into COS7 cells using FuGENE (Roche) as previously described (31,34,74). Extracted proteins were separated on a 15% sodium dodecyl sulfate polyacrylamide gel electrophoresis gel, transferred to nitrocellulose membranes (BioRad), incubated with primary antibody [anti-V5 (1:10 000), secreted alkaline phosphatase (1:5000) or α-tubulin (1:10 000), (AbCam)] and subsequently with anti-mouse or anti-rabbit IgG-HRP [1:5000 (Jackson Laboratories)]. After chemoluminescent antibody detection, images were analyzed using ImageJ and for quantification, protein amounts were normalized to alpha-tubulin and secreted alkaline phosphatase (SEAP) levels in the cytosolic and media fractions, respectively. For luciferase assays, U2OS cells cultured in 24-well plates until 80% confluency were transfected using FuGENE with either wild-type or variant *GDF6*, the luciferase reporter gene under the control of a 2x*BRE* (BMP-responsive element) and a pRL-SV40 encoding *Renilla* luciferase. Cell lysates were collected 48 h post-transfection and luciferase activity quantified [Dual luciferase kit (Promega)] in quadruplicate assays performed on three separate occasions.

Murine analysis

Gdf6 mutant mice [*Gdf6*^{tm1Lex} (MGI: 3604391)], previously genotyped by sequencing ear-notch derived DNA (31), underwent full-field ERGs at 14–23 months of age with the Espion E2 system (Diagnosys LLC). Briefly, mice were dark-adapted overnight and responses to a white flash (6500°K xenon) were recorded at incremental intensities (19 steps, range: −5.22–2.86 log candela s/m^2). After photopic adaptation (30 candela/m^2), photopic intensity responses were recorded (11 steps, range: −1.22–2.86 log candela s/m^2), followed by photopic flicker ERGs, all as previously described (75). For TUNEL analysis, timed pregnancies were used to generate E18 embryos that were collected from euthanized pregnant females, with dissected eyes preserved in PFA, paraffin

embedded and sectioned. Apoptosis was detected by terminal deoxytransferase-mediated dUTP nick end-labeling [TUNEL detection kit (Roche); counterstaining Hoechst 33258 (Invitrogen)], with standard positive (DNase incubation) and negative controls (omission of TdT from reaction buffer). Six retinal sections ($\geq$100 μm apart) were imaged from each eye with confocal microscopy (Carl Zeiss) to quantify the TUNEL-positive cells per section (statistical analysis, Student's *t* test). All murine procedures and husbandry were approved by the University of Alberta Animal Policy and Welfare Committee.

Zebrafish analysis

Adult *gdf6a*$^{s327/s327}$ and *gdf6a*$^{+/+}$ zebrafish and enucleated eyes were photographed under a Leica stereomicroscope, with genotyping performed by direct sequencing. Enucleated eyes were fixed and cryo-preserved using standard methods prior to immunohistochemistry (full details will be available on request). Briefly, 10 μm histological sections were blocked with goat serum, labeled with rhodamine–phalloidin or primary antibodies [to either red/green double cones (zpr1) or GFAP (zfr1)] and fluorescently conjugated secondary antibodies (Invitrogen), and counterstained (TO-PRO-3 or propidium iodide). Images were collected using confocal microscopy and pseudocoloured (Zeiss LSM 700 on Axio Observer.Z1). To investigate the effect of P7C3, embryos were treated from 5 to 28 hpf with either 0.01 μM P7C3, 0.1 μM P7C3 or DMSO. The level of apoptosis at 28 hpf in dissected eyes was determined using anti-active caspase-3 antibody staining (BD Pharmingen) and confocal microscopy (as above). Since *gdf6a* mutants do not have an observable phenotype at 28 hpf, genotypes were determined by PCR and sequencing. ANOVA analysis was performed with significance values at *P*-value of $<$0.00001. For the visual background mediated adaptation assays (VBA), embryos were treated with P7C3 from 5 to 48 hpf (the period during which apoptosis has been detected in *gdf6a*$^{-/-}$ mutants), transferred to embryo media until they reached 7 dpf, at which point they were individually scored for pigmentation (76). For OMR recordings, the distance travelled by individual larvae in response to a visual stimulus was measured (77) with *gdf6a*$^{-/-}$ mutants and non-mutant siblings treated with 0.01 μM P7C3 as described above.

SUPPLEMENTARY MATERIAL

Supplementary Material is available at *HMG* online.

ACKNOWLEDGEMENTS

We are very grateful to the patients and families whose participation made this research possible. We thank Ming Ye, Erin Strachan, Hao Wang, Aleah McCorry, Sharee Kuny and Frauke Coppieters for technical assistance; Aleah McCorry and Erin Wilson for zebrafish husbandry, Drs Michael Underhill and Laszlo Patthy for helpful advice and Drs Rod Bremner and Tsutomu Kume for critically reviewing the manuscript.

Conflict of Interest statement. None declared.

FUNDING

This work was supported by grants from Foundation Fighting Blindness Canada (A.J.W. and O.J.L.), Canadian Institutes of Health Research (O.J.L.), National Sciences and Engineering Research Council of Canada (W.T.A.), Funds for Scientific Research (E.D.B.), as well as the Canada Research Chair Program (A.J.W. and O.J.L.).

REFERENCES

1. Arnold, S.J. and Robertson, E.J. (2009) Making a commitment: cell lineage allocation and axis patterning in the early mouse embryo. *Nat. Rev. Mol. Cell Biol.*, **10**, 91–103.
2. Lie, D.C., Colamarino, S.A., Song, H.J., Desire, L., Mira, H., Consiglio, A., Lein, E.S., Jessberger, S., Lansford, H., Dearie, A.R. *et al.* (2005) Wnt signalling regulates adult hippocampal neurogenesis. *Nature*, **437**, 1370–1375.
3. Mathura, J.R. Jr., Jafari, N., Chang, J.T., Hackett, S.F., Wahlin, K.J., Della, N.G., Okamoto, N., Zack, D.J. and Campochiaro, P.A. (2000) Bone morphogenetic proteins-2 and -4: negative growth regulators in adult retinal pigmented epithelium. *Invest. Ophthalmol. Vis. Sci.*, **41**, 592–600.
4. Chang, H., Brown, C.W. and Matzuk, M.M. (2002) Genetic analysis of the mammalian transforming growth factor-beta superfamily. *Endocr. Rev.*, **23**, 787–823.
5. Massague, J., Blain, S.W. and Lo, R.S. (2000) TGFbeta signaling in growth control, cancer, and heritable disorders. *Cell*, **103**, 295–309.
6. Massague, J. and Chen, Y.G. (2000) Controlling TGF-beta signaling. *Genes Dev.*, **14**, 627–644.
7. Hogan, B.L. (1996) Bone morphogenetic proteins: multifunctional regulators of vertebrate development. *Genes Dev.*, **10**, 1580–1594.
8. Chang, C. and Hemmati-Brivanlou, A. (1999) Xenopus GDF6, a new antagonist of noggin and a partner of BMPs. *Development*, **126**, 3347–3357.
9. Israel, D.I., Nove, J., Kerns, K.M., Moutsatsos, I.K. and Kaufman, R.J. (1992) Expression and characterization of bone morphogenetic protein-2 in Chinese hamster ovary cells. *Growth Factors*, **7**, 139–150.
10. Aono, A., Hazama, M., Notoya, K., Taketomi, S., Yamasaki, H., Tsukuda, R., Sasaki, S. and Fujisawa, Y. (1995) Potent ectopic bone-inducing activity of bone morphogenetic protein-4/7 heterodimer. *Biochem. Biophys. Res. Commun.*, **210**, 670–677.
11. Miyazono, K., Maeda, S. and Imamura, T. (2005) BMP receptor signaling: transcriptional targets, regulation of signals, and signaling cross-talk. *Cytokine Growth Factor Rev.*, **16**, 251–263.
12. Zhang, Y.E. (2009) Non-Smad pathways in TGF-beta signaling. *Cell Res.*, **19**, 128–139.
13. Urist, M.R. (1965) Bone: formation by autoinduction. *Science*, **150**, 893–899.
14. Hogan, B.L. (1996) Bone morphogenetic proteins in development. *Curr. Opin. Genet. Dev.*, **6**, 432–438.
15. Graff, J.M. (1997) Embryonic patterning: to BMP or not to BMP, that is the question. *Cell*, **89**, 171–174.
16. Yang, X.J. (2004) Roles of cell-extrinsic growth factors in vertebrate eye pattern formation and retinogenesis. *Semin. Cell Dev. Biol.*, **15**, 91–103.
17. Koshiba-Takeuchi, K., Takeuchi, J.K., Matsumoto, K., Momose, T., Uno, K., Hoepker, V., Ogura, K., Takahashi, N., Nakamura, H., Yasuda, K. *et al.* (2000) Tbx5 and the retinotectum projection. *Science*, **287**, 134–137.
18. Sasagawa, S., Takabatake, T., Takabatake, Y., Muramatsu, T. and Takeshima, K. (2002) Axes establishment during eye morphogenesis in Xenopus by coordinate and antagonistic actions of BMP4, Shh, and RA. *Genesis*, **33**, 86–96.
19. Lupo, G., Liu, Y., Qiu, R., Chandraratna, R.A., Barsacchi, G., He, R.Q. and Harris, W.A. (2005) Dorsoventral patterning of the Xenopus eye: a collaboration of Retinoid, Hedgehog and FGF receptor signaling. *Development*, **132**, 1737–1748.
20. Rissi, M., Wittbrodt, J., Delot, E., Naegeli, M. and Rosa, F.M. (1995) Zebrafish Radar: a new member of the TGF-beta superfamily defines dorsal regions of the neural plate and the embryonic retina. *Mech. Dev.*, **49**, 223–234.

21. Gosse, N.J. and Baier, H. (2009) An essential role for Radar (Gdf6a) in inducing dorsal fate in the zebrafish retina. *Proc. Natl Acad. Sci. USA*, **106**, 2236–2241.
22. French, C.R., Erickson, T., French, D.V., Pilgrim, D.B. and Waskiewicz, A.J. (2009) Gdf6a is required for the initiation of dorsal-ventral retinal patterning and lens development. *Dev. Biol.*, **333**, 37–47.
23. den Hollander, A.I., Roepman, R., Koenekoop, R.K. and Cremers, F.P. (2008) Leber congenital amaurosis: genes, proteins and disease mechanisms. *Prog. Retin. Eye Res.*, **27**, 391–419.
24. Sohocki, M.M., Sullivan, L.S., Mintz-Hittner, H.A., Birch, D., Heckenlively, J.R., Freund, C.L., McInnes, R.R. and Daiger, S.P. (1998) A range of clinical phenotypes associated with mutations in CRX, a photoreceptor transcription-factor gene. *Am. J. Hum. Genet.*, **63**, 1307–1315.
25. Morimura, H., Fishman, G.A., Grover, S.A., Fulton, A.B., Berson, E.L. and Dryja, T.P. (1998) Mutations in the RPE65 gene in patients with autosomal recessive retinitis pigmentosa or leber congenital amaurosis. *Proc. Natl Acad. Sci. USA*, **95**, 3088–3093.
26. den Hollander, A.I., Johnson, K., de Kok, Y.J., Klebes, A., Brunner, H.G., Knust, E. and Cremers, F.P. (2001) CRB1 has a cytoplasmic domain that is functionally conserved between human and *Drosophila*. *Hum. Mol. Genet.*, **10**, 2767–2773.
27. den Hollander, A.I., Koenekoop, R.K., Yzer, S., Lopez, I., Arends, M.L., Voesenek, K.E., Zonneveld, M.N., Strom, T.M., Meitinger, T., Brunner, H.G. *et al.* (2006) Mutations in the CEP290 (NPHP6) gene are a frequent cause of Leber congenital amaurosis. *Am. J. Hum. Genet.*, **79**, 556–561.
28. Perrault, I., Hanein, S., Gerber, S., Barbet, F., Ducroq, D., Dollfus, H., Hamel, C., Dufier, J.L., Munnich, A., Kaplan, J. *et al.* (2004) Retinal dehydrogenase 12 (RDH12) mutations in leber congenital amaurosis. *Am. J. Hum. Genet.*, **75**, 639–646.
29. Cideciyan, A.V., Hauswirth, W.W., Aleman, T.S., Kaushal, S., Schwartz, S.B., Boye, S.L., Windsor, E.A., Conlon, T.J., Sumaroka, A., Pang, J.J. *et al.* (2009) Human RPE65 gene therapy for Leber congenital amaurosis: persistence of early visual improvements and safety at 1 year. *Hum. Gene Ther.*, **20**, 999–1004.
30. Ashtari, M., Cyckowski, L.L., Monroe, J.F., Marshall, K.A., Chung, D.C., Auricchio, A., Simonelli, F., Leroy, B.P., Maguire, A.M., Shindler, K.S. *et al.* (2011) The human visual cortex responds to gene therapy-mediated recovery of retinal function. *J. Clin. Invest.*, **121**, 2160–2168.
31. Asai-Coakwell, M., French, C.R., Ye, M., Garcha, K., Bigot, K., Perera, A.G., Staehling-Hampton, K., Mema, S.C., Chanda, B., Mushegian, A. *et al.* (2009) Incomplete penetrance and phenotypic variability characterize Gdf6-attributable oculo-skeletal phenotypes. *Hum. Mol. Genet.*, **18**, 1110–1121.
32. Galvin, J.A., Fishman, G.A., Stone, E.M. and Koenekoop, R.K. (2005) Clinical phenotypes in carriers of Leber congenital amaurosis mutations. *Ophthalmology*, **112**, 349–356.
33. Gonzalez-Rodriguez, J., Pelcastre, E.L., Tovilla-Canales, J.L., Garcia-Ortiz, J.E., Amato-Almanza, M., Villanueva-Mendoza, C., Espinosa-Mattar, Z. and Zenteno, J.C. (2010) Mutational screening of CHX10, GDF6, OTX2, RAX and SOX2 genes in 50 unrelated microphthalmia-anophthalmia-coloboma (MAC) spectrum cases. *Br J Ophthalmol*, **94**, 1100–1104.
34. Ye, M., Berry-Wynne, K.M., Asai-Coakwell, M., Sundaresan, P., Footz, T., French, C.R., Abitbol, M., Fleisch, V.C., Corbett, N., Allison, W.T. *et al.* (2010) Mutation of the bone morphogenetic protein GDF3 causes ocular and skeletal anomalies. *Hum. Mol. Genet.*, **19**, 287–298.
35. Tassabehji, M., Fang, Z.M., Hilton, E.N., McGaughran, J., Zhao, Z., de Bock, C.E., Howard, E., Malass, M., Donnai, D., Diwan, A. *et al.* (2008) Mutations in GDF6 are associated with vertebral segmentation defects in Klippel-Feil syndrome. *Hum. Mutat.*, **29**, 1017–1027.
36. Zilberberg, L., ten Dijke, P., Sakai, L.Y. and Rifkin, D.B. (2007) A rapid and sensitive bioassay to measure bone morphogenetic protein activity. *BMC Cell Biol.*, **8**, 41.
37. Picker, A., Cavodeassi, F., Machate, A., Bernauer, S., Hans, S., Abe, G., Kawakami, K., Wilson, S.W. and Brand, M. (2009) Dynamic coupling of pattern formation and morphogenesis in the developing vertebrate retina. *PLoS Biol.*, **7**, e1000214.
38. Furuta, Y. and Hogan, B.L. (1998) BMP4 is essential for lens induction in the mouse embryo. *Genes Dev.*, **12**, 3764–3775.
39. Middeldorp, J. and Hol, E.M. (2011) GFAP in health and disease. *Prog. Neurobiol.*, **93**, 421–443.
40. Uchimoto, T., Nohara, H., Kamehara, R., Iwamura, M., Watanabe, N. and Kobayashi, Y. (1999) Mechanism of apoptosis induced by a lysosomotropic agent, L-leucyl-L-leucine methyl ester. *Apoptosis*, **4**, 357–362.
41. Pieper, A.A., Xie, S., Capota, E., Estill, S.J., Zhong, J., Long, J.M., Becker, G.L., Huntington, P., Goldman, S.E., Shen, C.H. *et al.* (2010) Discovery of a proneurogenic, neuroprotective chemical. *Cell*, **142**, 39–51.
42. Balm, P.H. and Groneveld, D. (1998) The melanin-concentrating hormone system in fish. *Ann. N. Y. Acad. Sci.*, **839**, 205–209.
43. Muto, A., Orger, M.B., Wehman, A.M., Smear, M.C., Kay, J.N., Page-McCaw, P.S., Gahtan, E., Xiao, T., Nevin, L.M., Gosse, N.J. *et al.* (2005) Forward genetic analysis of visual behavior in zebrafish. *PLoS Genet.*, **1**, e66.
44. Martinez-Morales, J.R., Del Bene, F., Nica, G., Hammerschmidt, M., Bovolenta, P. and Wittbrodt, J. (2005) Differentiation of the vertebrate retina is coordinated by an FGF signaling center. *Dev. Cell*, **8**, 565–574.
45. Nakayama, Y., Miyake, A., Nakagawa, Y., Mido, T., Yoshikawa, M., Konishi, M. and Itoh, N. (2008) Fgf19 is required for zebrafish lens and retina development. *Dev. Biol.*, **313**, 752–766.
46. Israel, D.I., Nove, J., Kerns, K.M., Kaufman, R.J., Rosen, V., Cox, K.A. and Wozney, J.M. (1996) Heterodimeric bone morphogenetic proteins show enhanced activity in vitro and in vivo. *Growth Factors*, **13**, 291–300.
47. Kim, J., Wu, H.H., Lander, A.D., Lyons, K.M., Matzuk, M.M. and Calof, A.L. (2005) GDF11 controls the timing of progenitor cell competence in developing retina. *Science*, **308**, 1927–1930.
48. Morcillo, J., Martinez-Morales, J.R., Trousse, F., Fermin, Y., Sowden, J.C. and Bovolenta, P. (2006) Proper patterning of the optic fissure requires the sequential activity of BMP7 and SHH. *Development*, **133**, 3179–3190.
49. Sakuta, H., Takahashi, H., Shintani, T., Etani, K., Aoshima, A. and Noda, M. (2006) Role of bone morphogenic protein 2 in retinal patterning and retinotectal projection. *J. Neurosci.*, **26**, 10868–10878.
50. Asai-Coakwell, M., French, C.R., Berry, K.M., Ye, M., Koss, R., Somerville, M., Mueller, R., van Heyningen, V., Waskiewicz, A.J. and Lehmann, O.J. (2007) GDF6, a novel locus for a spectrum of ocular developmental anomalies. *Am. J. Hum. Genet.*, **80**, 306–315.
51. McPherron, A.C., Lawler, A.M. and Lee, S.J. (1999) Regulation of anterior/posterior patterning of the axial skeleton by growth/differentiation factor 11. *Nat. Genet.*, **22**, 260–264.
52. Ramel, M.C. and Hill, C.S. (2012) Spatial regulation of BMP activity. *FEBS Lett*, **586**, 1929–1941.
53. Loeys, B., Lindsay, M., Schepers, D., Bolar, N., Doyle, J., Gallo, E., Fert-Bober, J., Kempers, M., Fishman, E., Chen, Y. *et al.* (2012) Loss-of-function mutations in TGFB2 cause Loeys–Dietz syndrome: towards solving the TGFb paradox in aortic aneurysmal disease. *Presented at The American Society of Human Genetics*, 2012, San Francisco. Abstract #80.
54. Beier, M., Franke, A., Paunel-Gorgulu, A.N., Scheerer, N. and Dunker, N. (2006) Transforming growth factor beta mediates apoptosis in the ganglion cell layer during all programmed cell death periods of the developing murine retina. *Neurosci. Res.*, **56**, 193–203.
55. Franke, A.G., Gubbe, C., Beier, M. and Duenker, N. (2006) Transforming growth factor-beta and bone morphogenetic proteins: cooperative players in chick and murine programmed retinal cell death. *J. Comp. Neurol.*, **495**, 263–278.
56. Trousse, F., Esteve, P. and Bovolenta, P. (2001) Bmp4 mediates apoptotic cell death in the developing chick eye. *J. Neurosci.*, **21**, 1292–1301.
57. Frank, D.B., Abtahi, A., Yamaguchi, D.J., Manning, S., Shyr, Y., Pozzi, A., Baldwin, H.S., Johnson, J.E. and de Caestecker, M.P. (2005) Bone morphogenetic protein 4 promotes pulmonary vascular remodeling in hypoxic pulmonary hypertension. *Circ. Res.*, **97**, 496–504.
58. Heger, J., Schiegnitz, E., von Waldthausen, D., Anwar, M.M., Piper, H.M. and Euler, G. (2010) Growth differentiation factor 15 acts anti-apoptotic and pro-hypertrophic in adult cardiomyocytes. *J. Cell Physiol.*, **224**, 120–126.
59. Kiyono, M. and Shibuya, M. (2003) Bone morphogenetic protein 4 mediates apoptosis of capillary endothelial cells during rat pupillary membrane regression. *Mol. Cell Biol.*, **23**, 4627–4636.
60. Ehata, S., Hanyu, A., Hayashi, M., Aburatani, H., Kato, Y., Fujime, M., Saitoh, M., Miyazawa, K., Imamura, T. and Miyazono, K. (2007) Transforming growth factor-beta promotes survival of mammary

carcinoma cells through induction of antiapoptotic transcription factor DEC1. *Cancer Res.*, **67**, 9694–9703.
61. Yokouchi, Y., Sakiyama, J., Kameda, T., Iba, H., Suzuki, A., Ueno, N. and Kuroiwa, A. (1996) BMP-2/-4 mediate programmed cell death in chicken limb buds. *Development*, **122**, 3725–3734.
62. Smith, A.J., Bainbridge, J.W. and Ali, R.R. (2009) Prospects for retinal gene replacement therapy. *Trends Genet.*, **25**, 156–165.
63. MacMillan, K.S., Naidoo, J., Liang, J., Melito, L., Williams, N.S., Morlock, L., Huntington, P.J., Estill, S.J., Longgood, J., Becker, G.L. *et al.* (2011) Development of proneurogenic, neuroprotective small molecules. *J. Am. Chem. Soc.*, **133**, 1428–1437.
64. Mihelec, M., Pearson, R.A., Robbie, S.J., Buch, P.K., Azam, S.A., Bainbridge, J.W., Smith, A.J. and Ali, R.R. (2011) Long-term preservation of cones and improvement in visual function following gene therapy in a mouse model of leber congenital amaurosis caused by guanylate cyclase-1 deficiency. *Hum. Gene Ther.*, **22**, 1179–1190.
65. Shimmi, O., Umulis, D., Othmer, H. and O'Connor, M.B. (2005) Facilitated transport of a Dpp/Scw heterodimer by Sog/Tsg leads to robust patterning of the *Drosophila* blastoderm embryo. *Cell*, **120**, 873–886.
66. Valera, E., Isaacs, M.J., Kawakami, Y., Izpisua Belmonte, J.C. and Choe, S. (2010) BMP-2/6 heterodimer is more effective than BMP-2 or BMP-6 homodimers as inductor of differentiation of human embryonic stem cells. *PLoS One*, **5**, e11167.
67. Balemans, W. and Van Hul, W. (2002) Extracellular regulation of BMP signaling in vertebrates: a cocktail of modulators. *Dev. Biol.*, **250**, 231–250.
68. Ehrlich, M., Horbelt, D., Marom, B., Knaus, P. and Henis, Y.I. (2011) Homomeric and heteromeric complexes among TGF-beta and BMP receptors and their roles in signaling. *Cell Signal*, **23**, 1424–1432.
69. Feng, X.H. and Derynck, R. (2005) Specificity and versatility in TGF-beta signaling through Smads. *Annu. Rev. Cell Dev. Biol.*, **21**, 659–693.
70. Sidi, S., Goutel, C., Peyrieras, N. and Rosa, F.M. (2003) Maternal induction of ventral fate by zebrafish radar. *Proc. Natl Acad. Sci. USA*, **100**, 3315–3320.
71. Bakrania, P., Efthymiou, M., Klein, J.C., Salt, A., Bunyan, D.J., Wyatt, A., Ponting, C.P., Martin, A., Williams, S., Lindley, V. *et al.* (2008) Mutations in BMP4 cause eye, brain, and digit developmental anomalies: overlap between the BMP4 and hedgehog signaling pathways. *Am. J. Hum. Genet.*, **82**, 304–319.
72. Reis, L.M., Tyler, R.C., Schilter, K.F., Abdul-Rahman, O., Innis, J.W., Kozel, B.A., Schneider, A.S., Bardakjian, T.M., Lose, E.J., Martin, D.M. *et al.* (2011) BMP4 loss-of-function mutations in developmental eye disorders including SHORT syndrome. *Hum. Genet.*, **130**, 495–504.
73. Zhang, X., Li, S., Xiao, X., Jia, X., Wang, P., Shen, H., Guo, X. and Zhang, Q. (2009) Mutational screening of 10 genes in Chinese patients with microphthalmia and/or coloboma. *Mol. Vis.*, **15**, 2911–2918.
74. Ploger, F., Seemann, P., Schmidt-von Kegler, M., Lehmann, K., Seidel, J., Kjaer, K.W., Pohl, J. and Mundlos, S. (2008) Brachydactyly type A2 associated with a defect in proGDF5 processing. *Hum. Mol. Genet.*, **17**, 1222–1233.
75. Gilmour, G.S., Gaillard, F., Watson, J., Kuny, S., Mema, S.C., Bonfield, S., Stell, W.K. and Sauve, Y. (2008) The electroretinogram (ERG) of a diurnal cone-rich laboratory rodent, the Nile grass rat (Arvicanthis niloticus). *Vis. Res.*, **48**, 2723–2731.
76. Fleisch, V.C. and Neuhauss, S.C. (2006) Visual behavior in zebrafish. *Zebrafish*, **3**, 191–201.
77. Orger, M.B., Gahtan, E., Muto, A., Page-McCaw, P., Smear, M.C. and Baier, H. (2004) Behavioral screening assays in zebrafish. *Methods Cell Biol.*, **77**, 53–68.